

IHTC14-22742

## EXPERIMENTAL STUDY ON A COMPACT METHANOL-FUELED REFORMER WITH HEAT REGENERATION USING CERAMIC HONEYCOMB

**Yasuhiro RAI**

Dept. of Mech. Eng. & Sci., Kyoto Univ.  
Kyoto, JAPAN

**Kazuya TATSUMI**

Dept. of Mech. Eng. & Sci., Kyoto Univ.  
Kyoto, JAPAN

**Kazuyoshi NAKABE**

Dept. of Mech. Eng. & Sci., Kyoto Univ.  
Kyoto, JAPAN

### ABSTRACT

On the way to a new era of our society which will be based on hydrogen energy, it is needed to develop on-site hydrogen production systems to cover current insufficient infrastructures of hydrogen supply network systems. For this, a highly efficient compact reformer can be one of the most suitable solutions for on-site production of hydrogen which is supplied to distributed electric power-generation systems. But, the local and overall energy balance in the reformer should be precisely controlled since the reforming reaction processes of hydrocarbon fuels are very sensitive to reaction temperature in the reformer. For smaller reformers, in particular, the amount of heat loss through the outer surfaces is large enough to dominate the reactions. An appropriate way for thermal energy management, therefore, is necessary to accomplish highly efficient reformers. For these backgrounds, a compact tubular-typed fuel reformer was fabricated in this study, and was applied to produce hydrogen from methanol, focusing on the partial oxidation reaction (POR). The reformer was composed of a stainless steel pipe as the reactor exterior and ceramic honeycomb blocks inserted in two locations of the reactor. The honeycomb blocks are expected to assist the reforming reactions and transfer the thermal energy of the exhaust gas to the reaction region, acting as a heat regenerator. The upstream-side honeycomb block was aimed to perform an effective heat exchange from the reactor wall to the reactant gas. By inserting the block, the reforming reaction became stable at right after the block. The maximum hydrogen production was achieved in the condition of equivalence ratio, around 3.5. The other honeycomb block was inserted in the downstream of the reaction zone to convert the thermal energy of exhaust gas to radiation energy which can be

transferred to the upstream reaction region. Comparing to the case without the downstream-side block, the temperature of the reaction region became higher. Gas temperatures in the downstream region, on the other hand, became lower. Methanol conversion ratio and hydrogen production ratio enhanced due to the higher temperature at the reaction region. These results indicate that the thermal energy possessed by the exhaust gas was regenerated in the reaction region by the downstream-side honeycomb block and contributes to enhance the efficiency of the fuel reformer.

### 1. INTRODUCTION

Hydrogen, which is called one of the most promising energy sources, can be used for highly efficient energy systems such as fuel cells and hydrogen engines. Although large-scale industrial process of hydrogen production has been established in chemical plants, time is required until the infrastructures of hydrogen distributions and storages are developed in civil life. Meanwhile, on-site hydrogen production will be crucially required for future distributed power supplying systems. Therefore, it is essential to develop a compact fuel reformer which is able to apply for variety of fuels and wide range of fuel purity. It is reported that the thermal condition of the reformer greatly affects the reforming performance in either case: with and without catalyst [1, 2]. Therefore, temperature control of the reformer will help improving the reformer effectiveness, start-up characteristic, response and the reduction of undesired exhausts such as soot or CO [3-6].

By considering the social and technical trend, bio-fuels may be one of the options of hydrogen carriers. Also, in the future, low purified fuel may be used as a reforming fuel due to

energy resource depletion. For such a low energy density fuel, it is more important to design fuel reformer considering heat energy management. When it comes to relatively small-sized compact fuel reformer, this consideration is more important, since heat release to the out of the system will be dominant due to its large surface area to volume ratio.

Okuyama et al. [7] reported that by applying heat regeneration by porous media which works as a radiant converter, it is possible to stabilize super-fuel-rich flame. This porous radiant converter efficiently converts the enthalpy of exhaust gas penetrating through the porous media and realizes energy regeneration to the upstream region of the reactor.

In the authors' previous studies [8, 9], partial oxidation reaction (POR) of methanol was studied in terms of temperature control, and it was reported that temperature greatly affects the efficiency of the reformer. In this paper, results of a prototype tubular-typed reformer using heat regeneration by ceramic honeycomb are reported. Methanol was used as fuel in the both previous and present experiments. Alcoholic fuel is relatively easy to transport and store since it is chemically stable and is in liquid phase under atmospheric temperature and pressure. It is, therefore, considered to be suitable to compact energy supply systems with an output of several kilo watts [10]. No catalyst was mounted on the reformer in the studies. As the initial step of evaluating the reformer, the experiment was conducted without inserting the catalyst to separate the effects of the catalyst characteristics from those of temperature control. Reforming gas temperatures and exhaust gas components were monitored in the reformer. The effects of equivalence ratio and reactant flow rate on the reforming characteristics are discussed, mainly focusing on POR.

## 2. EXPERIMENTAL SETUP

Figure 1 illustrates the schematic and cross-sectional views of the reformer. As shown in the figure, the reformer was composed of two parts, i.e., the evaporator and reactor.

The evaporator was made of a galvanized steel pipe with inner diameter and length of 28mm and 200mm, respectively. A fuel injection port was located at the side surface, on which an injector with electric valve was mounted. An electrical rectangular signal was sent from a function generator (Yokogawa; WE500, WE7281) to this injector to control the valve opening. Flow rate of the fuel jet was, therefore, controlled by adjusting the frequency and duty ratio of the electrical signal to a certain value. An air supply port was set at the upstream end of the evaporator. Air supplied to this port was provided from a compressor, and the flow rate was controlled by rotameter with needle valve (Kofloc; RK1250). In the upstream and downstream areas adjacent to the fuel supply port, electric band heaters (Sakaguchi E.H. Voc.; BH3430) were wrapped around the evaporator pipe. This heater was powered by a voltage slider (Yamabishi; V-130-3) and heated the evaporator wall up to a specified temperature. Thus, the fuel injected from the fuel supply port impinged on the inner wall of the evaporator, and was vaporized there. The vaporized fuel

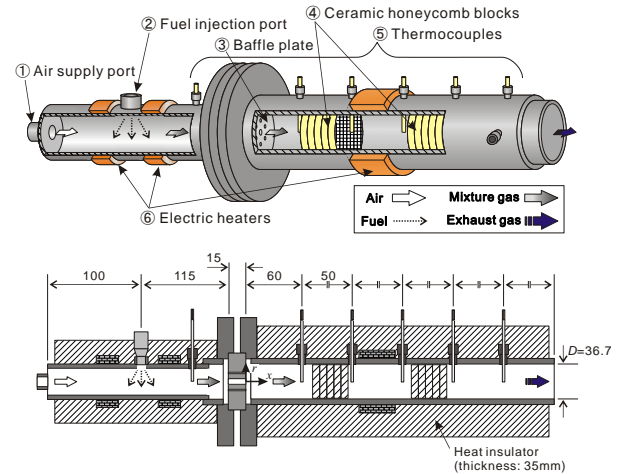


Fig. 1: Schematic view of the reformer (evaporator & reactor).

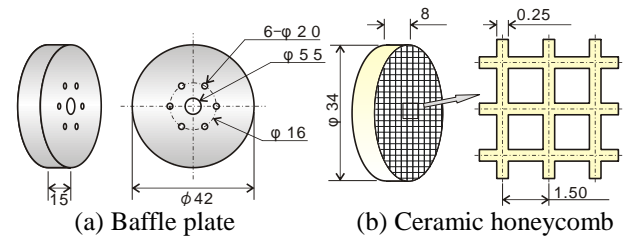


Fig. 2: Elements of the reformer.

Table 1: Flow rate conditions ( $Q_{\text{fuel}} = 0.092\text{cm}^3/\text{s}$ ).

$\phi$	3.0	3.5	4.0	4.5
$Q_{\text{air}}$ [L/min]	7.65	6.56	5.74	5.10

joining the air flowing from the upstream air supply port was then supplied to the reactor through a baffle plate.

As shown in Fig. 1, this baffle plate was located between the evaporator and reactor. Multiple holes were drilled in the 12mm-thick stainless steel disk. The configuration of the holes is shown in Fig. 2(a), i.e., a 5.5mm hole was located at the center of the disk and six holes with 2mm diameter surrounded the center one. This multi-hole baffle plate was expected to enhance the mixing between the vaporized fuel and air, and to prevent backfire from the reactor to the evaporator.

The reactor was made of a stainless steel pipe  $D = 36.7\text{mm}$  in inner diameter and 300mm in length. Ceramic honeycomb blocks shown in Fig. 2(b) were inserted in several locations in the reactor upstream region, which were expected to enhance heat transfer to the reactant gas and also to use heat regeneration from the exhaust gas by using radiative heat transfer. This 34-mm-in-diameter honeycomb was made of cordierite ceramic, and has mesh of cell number 300. Each block was 8mm-in-thickness, so that several blocks were put together by fireproof cement for desired thickness. Band heater (Watlow; MB01E1AB3005) was attached to the pipe sidewall at the location of  $3.1 \leq x/D \leq 4.3$ . This heater was powered by a voltage slider in the same way as those in the evaporator, and the pipe wall was preheated before the experiment started, so

that POR starts smoothly after reactants were supplied to the reactor.

Several loading ports were applied to the sidewalls of the evaporator and reactor at the locations shown in Fig. 1. These multiple ports can be used to insert measurement probes and possible multiple reactant supplying nozzles. Probes for temperature measurement made of K-type thermocouples were inserted into the pipe through these ports to measure the gas temperature at the axial center,  $T_{in}$ . To protect the exposed parts of the thermocouples from the flame and reactive gas, and also to prevent any catalysis effects, the thermocouples were coated by silica-particles. Thermocouples were also attached to the reactor exterior in order to measure the wall surface temperature,  $T_{ex}$ . Signals from the thermocouples were recorded by a personal computer through a digital multi-thermometer (Keyence; NR-1000). The sampling rate and accuracy of the temperature measurement was  $1s^{-1}$  and  $\pm 1^{\circ}C$ , respectively.

Gas sampling for gas component analysis was conducted by inserting a sampling probe into one of the loading ports. The probe was made of stainless steel tube, 3mm in outer diameter, to which a 0.3mm hole was applied at the end in order to freeze the gaseous reaction. The position of the tip end was set at the reactor centerline, and the gas was collected by connecting the tube to a vacuum-collecting chamber. The collected gas was then supplied to a gas chromatograph (Shimadzu; GC-8A) through a filtering chamber packed with silica gel, by which water and unburned methanol were removed from the gas. A component detector on the basis of TCD (Thermal Conductivity Detector) method was applied to the gas chromatography. The column (Shinwa chem.; Shincarbon ST) mounted in the chromatograph oven was calibrated for  $H_2$ ,  $N_2$ ,  $O_2$ ,  $CO$ , and  $CO_2$  gases. Argon gas was used as the carrier gas.

### 3. EXPERIMENTAL CONDITIONS

In this study, we investigate how ceramic honeycomb blocks affect reforming reactions.

First, we inserted one honeycomb block with thickness of 40mm at the region of the reactor,  $1.8 \leq x/D \leq 2.9$  and investigated basic reforming characteristic of this fuel reformer without using heat regeneration. In this case, the honeycomb block will be expected to improve reforming efficiency and also maintain stable reaction under high equivalence ratio by increasing the heat transfer to the reactant gas; POR did not happen at all if honeycomb block was not inserted.

Secondly, another honeycomb block (40mm in length) was inserted downstream of the first block. The secondary block will be expected to play the role of heat regeneration, i.e., enthalpy of exhaust gas was absorbed by the secondary honeycomb when the exhaust gas penetrates through the honeycomb, and a portion of the enthalpy was regenerated to the upstream reaction region by radiative and conductive heat transfer. By using energy regeneration from the exhaust gas, the reforming efficiency can be increased. The secondary honeycomb block was inserted downstream of the first block with streamwise space of 58mm, which works as a reaction

region of POR. It was confirmed that enough space for reaction was needed to stabilize POR in this reformer. This is because the reaction speed of POR is very slow compare to the complete combustion reaction because of its fuel rich condition.

As described in the previous section, experiments were carried out with regard to POR of methanol. Table 1 shows the flow rate conditions of reactants. Fuel and air were both supplied to the reactor from the evaporator through the baffle plate.  $Q_{air}$  and  $Q_{fuel}$  are the volume flow rates of the air and fuel fed to the evaporator, respectively. Note that  $Q_{fuel}$  represents the volume flow rate of the fuel in liquid form.  $\phi$  is the equivalence ratio based on the complete oxidative reaction. The stoichiometric equivalence ratio of the POR, therefore, is  $\phi = 3$ . As shown in Table 1,  $Q_{fuel}$  was fixed to one condition in the present experiments, and  $Q_{air}$  was varied in the range of equivalence ratios,  $3.0 \leq \phi \leq 4.5$ .

The procedure applied in the reaction experiment is described as follows. The evaporator and reactor pipes were first heated by the electric band heaters so that the temperatures measured at the locations of  $x/D = -3.9$ , upstream of the baffle plate rear surface, and  $x/D = 3.0$  reached  $200^{\circ}C$  and  $550^{\circ}C$ , respectively. Then, the heaters attached to the reactor were turned off and the fuel and air were supplied to the reformer. Note that the heaters of the evaporator continued to be powered during the experiment and the temperature inside the evaporator was kept at about  $150^{\circ}C$ .

## 4. RESULTS AND DISCUSSION

### 4.1 Parameters for evaluation of reformer performance

In the present study, the quantity of the consumed methanol cannot be measured directly due to the silica gel chamber, which collects water and unreacted methanol. Therefore, these quantities were estimated from the concentrations of the other gases included in the exhaust gas. Since the summation of the analyzed concentrations of  $H_2$ ,  $N_2$ ,  $O_2$ ,  $CO$  and  $CO_2$  in the exhaust gas was  $100 \pm 2\%$ , the major components of the gas was expected to be these five species plus water and unreacted methanol that were collected by the silica gel chamber. When paying attention to the carbon atoms, the components possessing carbon atoms among the products are  $CO$ ,  $CO_2$  and unreacted methanol. Therefore, the quantity of the consumed methanol can be calculated using the concentrations of  $CO$  and  $CO_2$  in the exhaust gas. Therefore, the methanol conversion ratio,  $\alpha$ , is defined as follows:

$$\begin{aligned} \alpha &\equiv \frac{M_{CH_3OH, consumed}}{M_{CH_3OH, supplied}} = \frac{M_{CO} + M_{CO_2}}{M_{CH_3OH, supplied}} \\ &= \frac{Y_{CO} + Y_{CO_2}}{Y_{N_2}} \times \frac{M_{N_2}}{M_{CH_3OH, supplied}} \end{aligned} \quad (1)$$

where  $M_X$  is the molar flow rate of the  $X$  component in the exhaust gas, and  $Y_X$  is the  $X$ 's concentration.

To evaluate the production efficiency of each component, the production rate of component  $X$  against 1mol of methanol supplied,  $\xi_X$ , is defined as follows:

$$\xi_x \equiv \frac{M_x}{M_{\text{CH}_3\text{OH}, \text{supplied}}} = \frac{(Y_x / Y_{\text{N}_2}) M_{\text{N}_2}}{M_{\text{CH}_3\text{OH}, \text{supplied}}} \quad (2)$$

In calculating the production rate of  $\text{H}_2\text{O}$ ,  $\xi_{\text{H}_2\text{O}}$ , it is assumed that all hydrogen atoms originated from the reacted methanol are used in producing  $\text{H}_2$  and  $\text{H}_2\text{O}$ . Thus,  $\xi_{\text{H}_2\text{O}}$  can be obtained by the following equation:

$$\xi_{\text{H}_2\text{O}} = 2\alpha - \xi_{\text{H}_2} \quad (3)$$

As a ratio of POR to complete combustion of methanol, we define  $\text{H}_2$  production efficiency,  $\beta$ , as follows:

$$\beta \equiv \frac{M_{\text{H}_2}}{M_{\text{CH}_3\text{OH}, \text{consumed}}} = 2 \times \frac{M_{\text{H}_2}}{M_{\text{H}_2} + M_{\text{H}_2\text{O}}} \quad (4)$$

$\beta$  indicates how large amount of  $\text{H}_2$  was produced against 1mol of consumed methanol. Therefore, the relation between  $\beta$  and parameters defined above is as follows:

$$\beta = \frac{\xi_{\text{H}_2}}{\alpha} \quad (5)$$

As an index of exhaust gas performance of the reformer, we introduce CO selectivity,  $\gamma$ , defined as the following equation:

$$\gamma \equiv \frac{M_{\text{CO}}}{M_{\text{CO}} + M_{\text{CO}_2}} \quad (6)$$

#### 4.2 Reforming experiments without heat regeneration (First honeycomb block only; Case-1)

Figure 3 shows the streamwise temperature distributions in the cases without heat regeneration, i.e., honeycomb block is inserted in the reactor only at the upstream region. The ordinate indicates the temperature measured, and the abscissa indicates the dimensionless streamwise position  $x/D$  from the downstream surface of the baffle plate. Hatched region in the graph indicates the location of honeycomb block. The present fuel reformer was possible to operate under as wide conditions as of equivalence ratio between 3.0 and 4.5. In Fig. 3, temperature distributions show similar trend regardless of equivalence ratio. Distributions of  $T_{\text{in}}$  take its maximum value at  $x/D = 4.4$  and temperature decreases as moves to downstream. These temperature distributions infer that the reforming reaction started near at the outlet of the first honeycomb block, and that the main exothermic reaction took place at the region of  $3.0 \leq x/D \leq 5.7$ . At  $x/D > 5.7$ , temperature decreases as  $x/D$  increases, so that the exothermic reaction did not take place at the downstream region. The wall surface temperature,  $T_{\text{ex}}$ , which is plotted using an open symbol and a broken line, does not experience a sudden temperature increase as seen in  $T_{\text{in}}$  but corresponds moderately to the gas temperature,  $T_{\text{in}}$ . The most upstream surface temperature,  $T_{\text{ex}}$  monitored at  $x/D = 1.6$ , is a bit higher than the corresponding

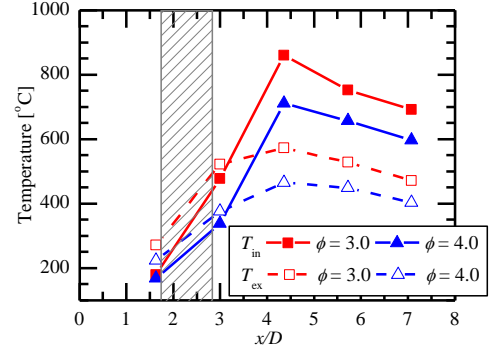


Fig. 3: Temperature distributions (Case-1).

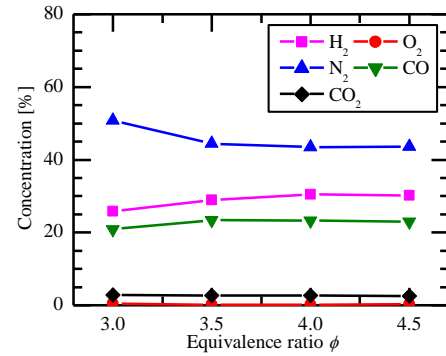


Fig. 4: Gas components concentration (Case-1).

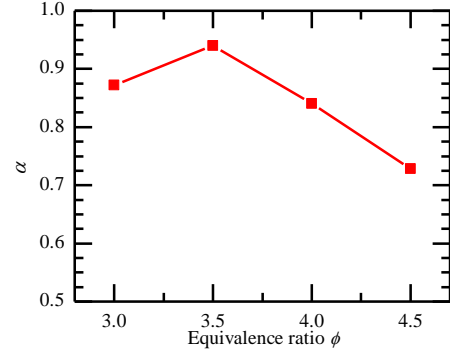


Fig. 5: Methanol conversion ratio,  $\alpha$  (Case-1).

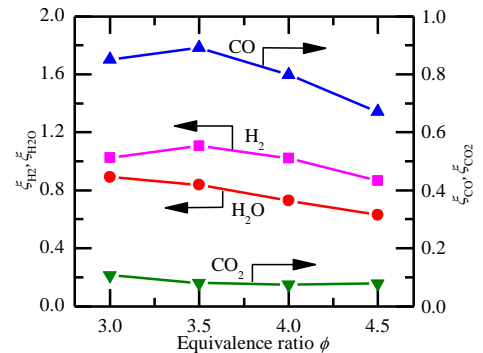


Fig. 6: Production ratio,  $\xi_x$ , for each species (Case-1).

gas temperature, which will be caused by heat conduction through the surface wall from the downstream side of the reactor. However,  $T_{ex}$  shows its maximum value at  $x/D = 4.4$  which is the same trend as  $T_{in}$ .

Comparing the temperature distributions in Fig. 3 with regard to equivalence ratio, maximum temperature level was obtained in the case of  $\phi = 3.0$ . The temperature level decreases as  $\phi$  increases. This is due to the fact that when  $\phi$  becomes small, the oxygen supply rate to methanol increases, which results in promoting the exothermic reaction of oxidation and increasing the temperature of the reforming gas.

Figure 4 shows the relation between the concentrations of components in the exhaust gas and equivalence ratio,  $\phi$ . The concentration of  $O_2$  is less than 0.5% in all cases indicating that the supplied  $O_2$  was totally consumed in the reaction. The concentration of  $H_2$  slightly increases as  $\phi$  increases in the region of  $\phi < 4.0$ . In terms of concentration, the best operating condition of this fuel reformer was seemed to be near the equivalence ratio,  $\phi = 4.0$ . However, since water and unreacted methanol were removed by the silica gel column when analyzing the exhaust gas components, the results of concentration does not show the accurate evaluation of the efficiency of the fuel reformer. For these reasons, we introduce the above-defined parameters; methanol conversion ratio,  $\alpha$ , and production ratio  $\xi_x$ .

Figure 5 shows the relation between methanol conversion ratio,  $\alpha$ , and equivalence ratio,  $\phi$ .  $\alpha$  takes its maximum value at  $\phi = 3.5$  and decreases as  $\phi$  increases. This is due to the fact that larger equivalence ratio represents fuel-rich condition, which means oxidation reaction lacks oxygen supply relative to smaller equivalence ratio conditions, which cause smaller methanol conversion ratio compared to smaller  $\phi$  conditions.

The production ratio,  $\xi_x$ , is shown in Fig. 6.  $\xi_{H_2}$  takes its maximum value at  $\phi = 3.5$ , and decreases in the region of  $\phi > 3.5$ . This trend is similar to the methanol conversion ratio,  $\alpha$  (cf. Fig. 5). This result indicates that the production efficiency of hydrogen is greatly affected by the methanol conversion ratio. Therefore, it is assumed that if it is possible to increase  $\alpha$  somehow, it may result in larger hydrogen production.

#### 4.3 Reforming experiments with heat regeneration (Two honeycomb blocks inserted; Case-2)

Figure 7 shows the temperature distributions of Case-2, which is the case applying heat regeneration by the secondary honeycomb block insertion. By comparison with Case-1 (cf. Fig. 3), temperature rise between two honeycomb blocks ( $3.0 \leq x/D \leq 4.4$ ) and temperature drop downstream of the secondary honeycomb block ( $x/D \geq 5.7$ ) were observed for all the equivalence ratio conditions. The temperature drop at the downstream of the secondary block was caused by absorption of exhaust gas enthalpy by the honeycomb. Thus, it was considered that a portion of the enthalpy was regenerated to the region between the two honeycomb blocks. The wall surface temperatures plotted with open symbols and broken lines follow the gas temperatures with a similar trend to Case 1. From these

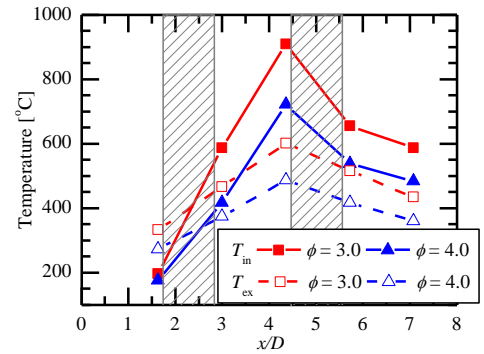


Fig. 7: Temperature distributions (Case-2).

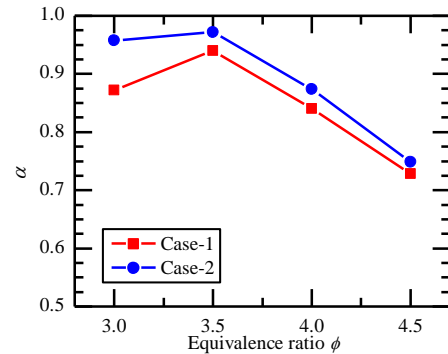


Fig. 8: Methanol conversion ratio,  $\alpha$  (Cases-1&2).

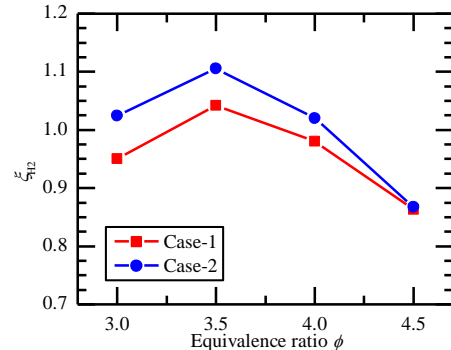


Fig. 9: Hydrogen production ratio,  $\xi$  (Cases-1&2).

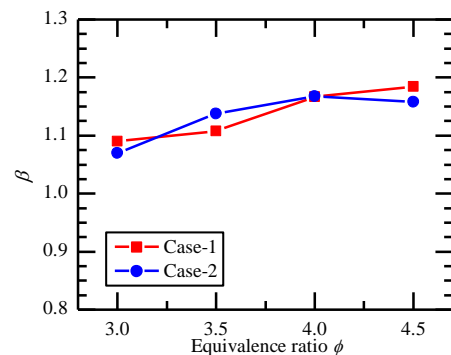


Fig. 10: Hydrogen production efficiency,  $\beta$  (Cases-1&2).

results of temperature distributions, the secondary honeycomb block was proved to work as a heat regenerator by absorbing the enthalpy of the exhaust gas.

Figures 8 and 9 show the comparison between Cases-1&2 of methanol conversion ratio,  $\alpha$ , and hydrogen production ratio,  $\xi_{H_2}$  plotted with regard to equivalence ratio,  $\phi$ . Methanol conversion ratio,  $\alpha$ , was improved in all the conditions of  $\phi$  by inserting the secondary honeycomb block. As the best case,  $\phi = 3.0$ ,  $\alpha$  was observed about 10% enhancement by inserting the secondary honeycomb block. It is assumed that the improvement in  $\alpha$  was caused by the temperature rise between the honeycomb blocks. Higher temperature is believed to enhance methanol decomposition reaction and resulted in higher conversion ratio.

Hydrogen production ratio,  $\xi_{H_2}$ , had a similar trend to  $\alpha$  as shown in Fig. 9.  $\xi_{H_2}$  was improved in all the conditions of  $\phi$ , and at most 8% improvement was observed for the case of  $\phi = 3.0$ . This improvement was mainly caused by the enhancement of  $\alpha$  which is an effect of heat regeneration by the secondary honeycomb block.

Figure 10 shows the hydrogen production efficiency,  $\beta$ , of both Cases-1&2. Both cases show the similar trend;  $\beta$  increases with  $\phi$ . This trend is due to the fact that smaller  $\phi$  results in higher temperature in the reformer as shown in Figs. 3&7, which accelerated the oxidation of hydrogen and produced more water rather hydrogen. From the view point of  $\beta$ , higher  $\phi$  results in much better performance, however, the total amount of hydrogen production is small, since higher  $\phi$  leads smaller  $\alpha$ .

Figure 11 shows the CO selectivity,  $\gamma$ , for both cases. From this graph,  $\gamma$  is not affected by  $\phi$  and does not have significant difference between Cases-1&2. Therefore, it is difficult by the present fuel reformer to reduce the amount of CO; CO reduction device or CO selective oxidation catalyst are needed for practical use.

## 5. CONCLUSIONS

In the present article, the methanol fuel reformer using heat regeneration by ceramic honeycomb was experimentally evaluated on the basis of the thermal and reaction characteristics. The major conclusions obtained are listed in the following.

1. An alcoholic-fuel reformer consisting of evaporator and reactor was fabricated and operated under the conditions of varying the equivalence ratio,  $\phi$ , in the range of  $3.0 \leq \phi \leq 4.5$ . Hydrogen production and a suitable temperature level for practical use were obtained by the reformer.
2. A better performance was obtained under the conditions of  $\phi = 3.5$ , which is fuel-rich condition compare to the stoichiometric value of POR,  $\phi = 3$ .
3. Production ratio of hydrogen is greatly affected by the methanol conversion ratio. Therefore, it is assumed that if it is possible to increase  $\alpha$ , it results in larger hydrogen production.
4. In the case with the secondary ceramic honeycomb (Case-2), higher conversion ratio was obtained for all  $\phi$  cases. This result suggests that ceramic honeycomb works as a heat regenerator in this reformer.

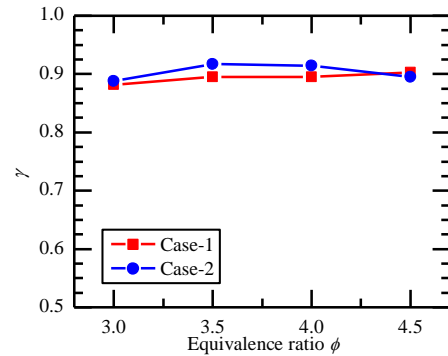


Fig. 11: CO selectivity (Cases-1&2).

## ACKNOWLEDGMENTS

This research was partially supported by Kyocera Corporation and Toyota Central R&D Labs., Inc. The authors also would like to acknowledge the great advice and help by the following colleagues: Mr. Keisuke Kuwabara, Mr. Daisuke Yamashita, and Mr. Masashi Kawabe.

## REFERENCES

1. B. Li, S. Kado and Y. Mukainakano, Temperature Profile of Catalyst Bed during Oxidative Steam Reforming of Methane over Pt-Ni Bimetallic Catalysts, *Applied Catalysis A*, General 304 (2006), pp. 62-71.
2. C. Pan, R. He and Q. Li, Integration of High Temperature PEM Fuel Cells with a Methanol Reformer, *J. Power Sources*, 145 (2005), pp. 392-398.
3. A. L. Dicks, Hydrogen Generation from Natural Gas for the Fuel Cell Systems of Tomorrow, *J. Power Sources*, 61 (1996), pp. 113-124.
4. H. Marsh and D. Thingarajan, *AIChE Ammonia Safety Symposium*, (1992).
5. M. Dunster and J. Korchnak, Production of Synthesis gas from Hydrocarbonaceous Feedstock, *Eur Patent No. 303438*, (1989).
6. T. Calcott and T. Deague, *US Patent No. 4 042 344*, (1977).
7. M. Okuyama, K. Hanamura, R. Echigo and H. Yoshida, Flame structure of super fuel-rich premixed flame, *Transactions of the Japan Society of Mechanical Engineers. B*, 61 (587), pp.2724-2730.
8. K. Tatsumi, K. Kuwabara, Y. Rai and K. Nakabe, Heat and Reaction Characteristics of Multistage Alcoholic-Fuel Reformer, *Proc. 18<sup>th</sup> Int'l Symp. Transport Phenomena (ISTP-18)*, (2007), pp. 847-854.
9. Y. Rai, K. Tatsumi, K. Kuwabara and K. Nakabe, Heat and Reaction Characteristics of Multistage Alcoholic-Fuel Reformer (2nd report: Velocity and Radical Chemiluminescence Measurements), *Proc. Int'l Conference on Power Engineering (ICOPE-09)*, (2009), pp. 2-271-276.
10. J. Larminie and A. Dicks, *Fuel Cell Systems Explained*, (2003), John Wiley & Sons Inc.